A variational framework for spatio-temporal smoothing of fluid motions

Nicolas Papadakis and Étienne Mémin

IRISA/INRIA, Campus de Beaulieu, 35042 Rennes Cedex, FRANCE
{Nicolas.Papadakis,Etienne.Memin}@irisa.fr

Abstract. In this paper, we introduce a variational framework derived from data assimilation principles in order to realize a temporal Bayesian smoothing of fluid flow velocity fields. The velocity measurements are supplied by an optical flow estimator. These noisy measurement are smoothed according to the vorticity-velocity formulation of Navier-Stokes equation. Following optimal control recipes, the associated minimization is conducted through an iterative process involving a forward integration of our dynamical model followed by a backward integration of an adjoint evolution law. Both evolution laws are implemented with second order non-oscillatory scheme. The approach is here validated on a synthetic sequence of turbulent 2D flow provided by Direct Numerical Simulation (DNS) and on a real world meteorological satellite image sequence depicting the evolution of a cyclone.

1 Introduction

The analysis and control of complex fluid flows is a major scientific issue. In that prospect, flow visualization and extraction of accurate kinetic or dynamical measurements are of the utmost importance. For several years, the study of dynamic structures and the estimation of dense velocity fields from fluid image sequences have received great attention from the computer vision community [3, 7, 8, 15, 18, 26]. Application domains range from experimental visualization in fluid mechanical to geophysical flow analysis in environmental sciences. In particular, accurate measurement of atmospheric flow dynamics is of the greatest importance for weather forecasting, climate prediction or analysis, etc...

The analysis of motion in such sequences is particularly challenging due to abrupt and sudden changes of the luminance function in image sequences. For these reasons, motion analysis techniques designed for computer vision application and quasi-rigid motions, are not well adapted in this context. Recently, methods for fluid-dedicated dense estimation have been proposed to characterize fluid motion [3–5, 12, 24, 25]. However, these motion estimators are still using only a small set of images and thus may suffer from a temporal inconsistency from frame to frame. The set of motion fields provided may not respect fluid mechanics conservation laws. The design of appropriate methods enabling to take into account the underlying physics of the observed flow constitutes a widely open domain of research. We are here interested in using the *vorticity-velocity* formulation of *Navier-Stokes* equations which describes accurately the evolution of vorticity transported by the flow for the filtering of noisy motion fields.

The approach we propose in this work is related to variational data assimilation principles used for instance in meteorology [1, 6, 23]. Such techniques enable, in the same spirit as a Kalman filter, a temporal smoothing along the whole image sequence. As does a Bayesian smoother, it combines a dynamical evolution law of state variables representing the target of interest with the whole set of available noisy measurements related to this target. Nevertheless, unlike Kalman filtering and stochastic Bayesian filtering approaches such as particle filtering, variational assimilation techniques allows to cope with state spaces of very large dimension.

The technique we devise allows us to incorporate in the whole set of motion fields a dynamical consistency along the image sequence. The approach is expressed as the minimization of a global spatio-temporal functional stemming from a Bayesian formulation. The optimization process is led through the introduction of an adjoint evolution model. This method has the advantage to provide an efficient numerical approximation of the gradient functional without resorting to the complete analytical expressions of Euler-Lagrange equations. This is particularly interesting when dealing with high order differential operators.

2 Data assimilation

2.1 Introduction

Data Assimilation is a technique related to optimal control theory which allows estimating over time the state of a system of variables of interest. This method enables a smoothing of the unknown variables according to an initial state of the system, a dynamic law and noisy measurements of the system's state. Let the vector of variables $\boldsymbol{X} \in \Xi$ represents the state of the system. The evolution of the system is assumed to be described through a (possibly non linear) differential dynamical model $\mathbb{M}$:

$$\begin{cases} \partial_t \boldsymbol{X} + \mathbb{M}(\boldsymbol{X}, U) = 0 \\ \boldsymbol{X}(t_0) = \boldsymbol{X}_0 \end{cases} \tag{1}$$

This system is monitored by a control variable $v = (U, \boldsymbol{X}_0)$ defined in control space P. This control variable may be set to the initial condition $\boldsymbol{X}_0$ and/or to any free parameters U of the evolution law.

We then assume that observations $Y \in O_{obs}$ are available. These observations may live in a different space (a reduced space for instance) from the state variable. We will nevertheless assume that there exists a differential operator $\mathbb{H}$, that goes from the variable space to the observation space. A least squares estimation of the control variable regarding the whole sequence of measurements available within a considered time range comes to minimize with respect to the control variable $v \in P$, a cost function of the following form:

$$J(v) = \frac{1}{2} \int_{t_0}^{t_f} ||Y - \mathbb{H}(\boldsymbol{X}(v))||^2 \, dt. \tag{2}$$

A first approach consists in computing the functional gradient through finite differences:

$$\nabla_v J \simeq \lim_{\epsilon \to 0} \frac{J(v + \epsilon e_k) - J(v)}{\epsilon},$$

where $\epsilon \in \mathbb{R}$ is an infinitesimal perturbation and $\{e_k, k = 1, \ldots, N\}$ denotes the unitary basis vectors of the control space of dimension N. Such a computation is

impractical for control space of large dimension since it requires N integrations of the evolution model for each required value of the gradient functional.

Adjoint models as introduced first in meteorology by Le Dimet and Talagrand in [6] authorize the computation of the gradient functional in a single backward integration of an adjoint variable. The value of this adjoint variable at the initial time provides the value of the gradient at the desired point. This first approach is widely used in environmental sciences for the analysis of geophysical flows [6, 23]. However, these methods rely on a perfect dynamical modeling of the system evolution. Such modeling seems to us irrelevant in image analysis since the different models on which we can rely on are usually inaccurate due for instance to 3D-2D projections, varying lighting conditions, completely unknown boundary conditions, etc ... Considering imperfect models, defined up to a Gaussian noise comes to an optimization problem where the control variable is constituted by the whole trajectory of the state variable. This is the kind of problem we are facing in this work.

2.2 Data assimilation with imperfect model

The ingredients of the new data assimilation problem are now composed by an imperfect dynamic model of the target system (without parameter U), an initialization of the system's state and an observation equation which relates the system variables to some measurements:

$$\begin{cases} \partial_t \boldsymbol{X} + \mathbb{M}(\boldsymbol{X}) = \boldsymbol{\eta}(\boldsymbol{x}, t) \\ \boldsymbol{X}(t_0) = \boldsymbol{X}_0 + \boldsymbol{\eta}_i(\boldsymbol{x}) \\ Y(t) = \mathbb{H}(\boldsymbol{X}) + \eta_o(\boldsymbol{x}, t), \end{cases} \tag{3}$$

where $\boldsymbol{\eta}$, $\boldsymbol{\eta}_i$ and η_o are time varying zero mean Gaussian noise vector functions. They are respectively associated to covariance matrices $Q(\boldsymbol{x}, t)$, $B(\boldsymbol{x}, \boldsymbol{x}')$ and $R(\boldsymbol{x}, t)$. The state variable $\boldsymbol{X}$ is defined on the image plan Ω. The noise functions represent the errors involved in the different components of the system (i.e model, initialization and measurement errors) and are assumed to be uncorrelated in time. The system of equations (3) could be specified describing the three Gaussian conditional probability densities $p(\boldsymbol{X}|\boldsymbol{X}(0))$, $p(\boldsymbol{X}(0)|\boldsymbol{X}_0)$ and $p(Y|\boldsymbol{X})$ which relates respectively the state trajectory $\boldsymbol{X}$ along time to the initial state value $\boldsymbol{X}(0)$, the initial state value to the initial condition $\boldsymbol{X}_0$ and Y, and the complete set of measurements to the state $\boldsymbol{X}$. As in any stochastic filtering problem, we aim at estimating the conditional expectation of the state trajectory given the whole set of available observations. As all the pdf involved here are Gaussian, it becomes estimating the mode of the *a posteriori* distribution $p(\boldsymbol{X}|Y, \boldsymbol{X}_0)$.

Penalty function The goal is thus to minimize the new functional:

$$J(\boldsymbol{X}) = \frac{1}{2}\int_{t_0}^{t_f} ||\partial_t \boldsymbol{X} + \mathbb{M}(\boldsymbol{X})||_Q^2 dt + \frac{1}{2}\,||\boldsymbol{X}(t_0) - \boldsymbol{X}_0||_B^2 + \frac{1}{2}\int_{t_0}^{t_f} ||Y - \mathbb{H}(\boldsymbol{X})||_R^2\, dt, \tag{4}$$

where the norms are the Mahalanobis distance defined by the inverse matrices associated to Q, B and R (the information matrices) and the dot product of

$L^2(\Omega)$. The minimization has to be done according to variable $\boldsymbol{X}$. It is the complete trajectory of the state variable that constitutes the control variable of the associated problem.

Minimization of the functional A minimizer $\boldsymbol{X}$ of functional J is also a minimizer of a perturbed function $J(\boldsymbol{X}+\beta\boldsymbol{\theta}(\boldsymbol{x},t))$, where $\boldsymbol{\theta}(\boldsymbol{x},t)$ belongs to a space of admissible function and β is a positive parameter. In other words, $\boldsymbol{X}$ must cancel out the directional derivative:

$$\delta J_{\boldsymbol{X}}(\boldsymbol{\theta}) = \lim_{\beta\to 0} \frac{dJ(\boldsymbol{X}+\beta\boldsymbol{\theta}(\boldsymbol{x},t))}{d\beta} = 0.$$

The functional J at point $\boldsymbol{X}+\beta\boldsymbol{\theta}(\boldsymbol{x},t))$ reads:

$$\begin{aligned} J = &\frac{1}{2}\int_{\Omega}(\boldsymbol{X}+\beta\boldsymbol{\theta}-\boldsymbol{X}_0)^\top B^{-1}(\boldsymbol{X}+\beta\boldsymbol{\theta}-\boldsymbol{X}_0)d\boldsymbol{x} \\ &+\frac{1}{2}\int_{\Omega,T}(\partial_t\boldsymbol{X}+\beta\partial_t\boldsymbol{\theta}+\mathbb{M}(\boldsymbol{X}+\beta\boldsymbol{\theta}))^\top Q^{-1}(\partial_t\boldsymbol{X}+\beta\partial_t\boldsymbol{\theta}+\mathbb{M}(\boldsymbol{X}+\beta\boldsymbol{\theta}))\,dtd\boldsymbol{x} \\ &+\frac{1}{2}\int_{\Omega,T}(Y-\mathbb{H}(\boldsymbol{X}+\beta\boldsymbol{\theta}))^\top R^{-1}(Y-\mathbb{H}(\boldsymbol{X}+\beta\boldsymbol{\theta}))dtd\boldsymbol{x}, \end{aligned} \tag{5}$$

where integration with respect to Ω denotes spatial integration on the image domain and subscript T stands for temporal integration between an initial time t_0 and a final instant t_f

Adjoint variable In order to perform an integration by part – to factorize this expression by $\boldsymbol{\theta}$ – we introduce an "adjoint variable" $\boldsymbol{\lambda}$ defined by:

$$\boldsymbol{\lambda} = Q^{-1}\left(\partial_t\boldsymbol{X}+\mathbb{M}(\boldsymbol{X})\right), \tag{6}$$

as well as *linear tangent operators* $\partial_{\boldsymbol{X}}\mathbb{M}$ and $\partial_{\boldsymbol{X}}\mathbb{H}$ defined by:

$$\lim_{\beta\to 0}\frac{d\mathbb{M}(\boldsymbol{X}+\beta\boldsymbol{\theta})}{d\beta} = \partial_{\boldsymbol{X}}\mathbb{M}\boldsymbol{\theta}. \tag{7}$$

Such linear operators correspond to the Gâteaux derivative at point $\boldsymbol{X}$ of the operators $\mathbb{M}$ and $\mathbb{H}$. Let us note that the derivative of a linear operator is the operator itself. By taking the limit $\beta\to 0$, and applying integrations by parts, we can get rid of the partial derivatives of the admissible function θ. We also have to introduce the adjoint operators $\partial_X\mathbb{M}^*$ and $\partial_X\mathbb{H}^*$ as compact notation of the integration by parts of the associated linear tangent operator. Considering the dot product $\langle\phi,\psi\rangle = \int_{\Omega,T}\phi(\boldsymbol{x},t)\psi(\boldsymbol{x},t)d\boldsymbol{x}dt$ associated to $L^2(\Omega,T\in[t_0,t_f])$ such operators are defined as:

$$\langle\partial_{\boldsymbol{X}}\mathbb{M}\boldsymbol{X}_1,\boldsymbol{X}_2\rangle_{\Xi} = \langle\boldsymbol{X}_1,\partial_{\boldsymbol{X}}\mathbb{M}^*\boldsymbol{X}_2\rangle_{\Xi} \qquad \langle\partial_{\boldsymbol{X}}\mathbb{H}\boldsymbol{X},Y\rangle_{O_{obs}} = \langle\boldsymbol{X},\partial_{\boldsymbol{X}}\mathbb{H}^*Y\rangle_{\Xi}. \tag{8}$$

Gathering all the elements we have so far, equation (5) can be rewritten as:

$$\begin{aligned} \lim_{\beta\to 0}\frac{dJ}{d\beta} = &\int_{\Omega,T}\boldsymbol{\theta}^\top\Big[(-\partial_t\boldsymbol{\lambda}+\partial_{\boldsymbol{X}}\mathbb{M}^*\boldsymbol{\lambda})-\partial_{\boldsymbol{X}}\mathbb{H}^*R^{-1}(Y-\mathbb{H}(\boldsymbol{X}))\Big]dtd\boldsymbol{x} \\ &+\int_{\Omega}\boldsymbol{\theta}^\top(\boldsymbol{x},t_0)\left[\left(B^{-1}(\boldsymbol{X}(\boldsymbol{x},t_0)-\boldsymbol{X}_0(\boldsymbol{x}))-\boldsymbol{\lambda}(\boldsymbol{x},t_0)\right)d\boldsymbol{x}'\right]d\boldsymbol{x} \\ &+\int_{\Omega}\boldsymbol{\theta}^\top(\boldsymbol{x},t_f)\boldsymbol{\lambda}(\boldsymbol{x},t_f)d\boldsymbol{x} = 0. \end{aligned} \tag{9}$$

Forward/backward equations Since the functional derivative must be null for any arbitrary independent admissible functions in the three integrals of expression (9), all the other members appearing in the three integral terms must be identically null. It follows a coupled system of forward and backward PDE's with initial and final conditions:

$$\boldsymbol{\lambda}(\boldsymbol{x}, t_f) = 0, \tag{10}$$

$$-\partial_t \boldsymbol{\lambda} + \partial_{\boldsymbol{X}} \mathbb{M}^* \boldsymbol{\lambda} = \partial_{\boldsymbol{X}} \mathbb{H}^* R^{-1} (Y - \mathbb{H}(\boldsymbol{X})), \tag{11}$$

$$\boldsymbol{\lambda}(\boldsymbol{x}, t_0) = \left(B^{-1} (\boldsymbol{X}(\boldsymbol{x}, t_0) - \boldsymbol{X}_0(\boldsymbol{x})) \right), \tag{12}$$

$$\partial_t \boldsymbol{X} + \mathbb{M}(\boldsymbol{X}) = Q\boldsymbol{\lambda}. \tag{13}$$

The forward equation (13) corresponds to the definition of the adjoint variable (6) and has been obtained introducing Q, the pseudo-inverse of Q^{-1} [1]. Let us remark that if the model is assumed to be perfect, we would have $Q = 0$ and retrieve the case of a perfect dynamical state model associated to an initial state control problem.

Otherwise, equation (10) constitutes an explicit end condition for the adjoint evolution model equation (11). This adjoint evolution model can be integrated backward from the end condition assuming the knowledge of an initial guess for $\boldsymbol{X}$ to compute the discrepancy $Y - \mathbb{H}(\boldsymbol{X})$. This backward integration provides the gradient of the associated functional. To perform this integration, an expression of the *adjoint evolution operator* is required. Let us recall that this operator is defined from an integration by part of the *linear tangent operator* associated to the evolution law operator. The analytic expression of such an operator is obviously not accessible in general. Nevertheless, it can be noticed that a discrete expression of this operator can be obtained from the discretization of the linear tangent operator. Thus, the adjoint of the linear tangent operator discretized as a matrix simply consists of the transpose of that matrix. Knowing a first solution of the adjoint variable, an initial update condition for the state variable can be obtained from (12) and a pseudo inverse expression of the covariance matrix B. From this initial condition, equation (13) can be finally integrated forward and supply a new right hand part for the adjoint equation (11) and so forth.

Incremental state function The previous system can be slightly modified to rely on an adequate initial guess for the state function. Considering a function of state increments linking the state function and an initial condition function, $\delta\boldsymbol{X} = \boldsymbol{X} - \boldsymbol{X}_0$, and linearizing the operator $\mathbb{M}$ around the initial condition function $\boldsymbol{X}_0$, as $\mathbb{M}(\boldsymbol{X}) = \mathbb{M}(\boldsymbol{X}_0) + \partial_{\boldsymbol{X}_0} \mathbb{M}(\delta\boldsymbol{X})$ enables to split equation (13) into two pde's with an explicit initial condition:

$$\boldsymbol{X}(\boldsymbol{x}, t_0) = \boldsymbol{X}_0(\boldsymbol{x}), \tag{14}$$

$$\partial_t \boldsymbol{X}_0 + \mathbb{M}(\boldsymbol{X}_0) = 0, \tag{15}$$

$$\partial_t \delta\boldsymbol{X} + \partial_{\boldsymbol{X}_0} \mathbb{M} \delta\boldsymbol{X} = Q\boldsymbol{\lambda}. \tag{16}$$

Combining equations (10-12) and (14-16) leads to the final tracking algorithm.

The method first consists of a forward integration of the initial condition $\boldsymbol{X}_0$ with the system's dynamical model equation (15). The current solution is then corrected by performing a backward integration (10, 11) of the adjoint variable.

The evolution of $\boldsymbol{\lambda}$ is guided by a discrepancy measure between the observation and the estimate: $Y - \mathbb{H}(\boldsymbol{X})$. The initial condition is then updated through equation (12) and a forward integration of the increment $\delta\boldsymbol{X}$ is realized through the equation (16). The overall process is iteratively repeated until convergence.

3 Application to fluid motion tracking

We aim here at applying the previous framework for a consistent tracking along time of fluid motion velocity fields. For fluid flows, the Navier-Stokes equation provides a universal general law for predicting the evolution of the flow. The purpose will be thus to incorporate into a data assimilation process such a dynamical model together with noisy velocity measurements.

3.1 Basic definitions

In this work, the formulation of the Navier-Stokes on which we will rely on uses the vorticity $\xi = \boldsymbol{\nabla}^{\perp} \cdot \boldsymbol{w} = v_x - u_y$ and on the divergence $\zeta = \boldsymbol{\nabla} \cdot \boldsymbol{w} = u_x + v_y$ of a bidimensional motion field $\boldsymbol{w} = [u, v]^{\top}$. The vorticity is related to the presence of a rotating motion, whereas the divergence is related to the presence of sinks and sources in a flow. Assuming $\boldsymbol{w}$ vanishes at infinity[1], the vector field is decomposed using the orthogonal Helmholtz decomposition, as a sum of two potential functions gradient $\boldsymbol{w} = \boldsymbol{\nabla}^{\perp}\Psi + \boldsymbol{\nabla}\Phi$. The stream function Ψ and the velocity potential Φ respectively correspond to the solenoidal and the irrotational part of the vector field $\boldsymbol{w}$. They are linked to the divergence and vorticity maps through two Poisson Equations: $\xi = \Delta\Psi$, $\zeta = \Delta\Phi$. Expressing the solution of both equations as a convolution product with the Green kernel $G = \frac{1}{2\pi}\ln(|x|)$ associated to the 2D Laplacian operator: $\Psi = G * \xi$, $\Phi = G * \zeta$, the whole velocity field can be recovered knowing its divergence and vorticity:

$$\boldsymbol{w} = \boldsymbol{\nabla}^{\perp} G * \xi + \boldsymbol{\nabla} G * \zeta. \tag{17}$$

This computation can be very efficiently implemented in the Fourier domain.

3.2 Fluid motion evolution equation

In order to consider a tractable expression of the Navier-Stokes equation for the tracking problem, we rely in this work on the 2D vorticity-velocity formulation of the 3D incompressible Navier-Stokes equation, as obtained in the shallow water model:

$$\partial_t \xi + \boldsymbol{w} \cdot \boldsymbol{\nabla}\xi + \xi\zeta - \nu\Delta\xi = 0. \tag{18}$$

This formulation states roughly that the vorticity is transported by the velocity field and is diffused along time. Modeling the vorticity divergence product as a zero mean Gaussian random variable, we end up with an imperfect 2D incompressible vorticity-velocity formulation.

Concerning the divergence map, it is more involved to exhibit any conservation law. We will assume here that it behaves like a noise. More precisely we will

[1] A divergence and curl free global transportation component is removed from the vector field. This field is estimated on the basis of a Horn and Schunck estimator associated to a high smoothing penalty [3].

assume that the divergence map is a function of a Gaussian random variable, X_t, with stationary increments (a Brownian motion) starting at points, $\boldsymbol{x}$. It can be shown through Ito formula and Kolmogorov's backward equation, that the expectation at time t of such a function, $u(t, \boldsymbol{x}) = \mathbb{E}[\zeta(X_t)]$ obeys to a heat equation [20]:

$$\begin{aligned} &\partial_t u - \nu_\zeta \Delta u = 0, \\ &u(0, \boldsymbol{x}) = \zeta(\boldsymbol{x}). \end{aligned} \tag{19}$$

According to this equation, we indeed make the assumption that the divergence at any time of the sequence is a solution of a heat equation (i.e. it can be recovered from a smoothing of the initial motion field divergence map with a Gaussian function of standard deviation $2\sqrt{\nu_\zeta}$).

As the curl and divergence maps completely determine the underlying velocity field, equations (18) and (19) allow us to write the following imperfect dynamical model for the fluid motion field:

$$\partial_t \begin{bmatrix} \xi \\ \zeta \end{bmatrix} + \underbrace{\begin{bmatrix} \boldsymbol{w} \cdot \boldsymbol{\nabla} - \nu_\xi \Delta & 0 \\ 0 & -\nu_\zeta \Delta \end{bmatrix}}_{\mathbb{M}(\xi,\zeta)} \begin{bmatrix} \xi \\ \zeta \end{bmatrix} = \boldsymbol{\eta}(t). \tag{20}$$

The noise function $\boldsymbol{\eta}(t)$ is a Gaussian random vector modeling the errors of our evolution law.

3.3 Fluid motion observations

With regards to the velocity measurements, we will assume that an observation motion field $\boldsymbol{w}_{obs}$ is available. This motion field can be provided by any dense motion estimator. In this work, a dense motion field estimator dedicated to fluid flows is used [3] to supply the velocity measurements. Taking the vorticity and divergence of these optical-flow motion fields as observation, provides measurements in the state variable space and consequently $\mathbb{H} = Id$.

4 Discretization of the vorticity-velocity equation

The discretization of the vorticity-velocity equation 18 must be done cautiously. In particular, the advective term $\boldsymbol{\nabla}\xi \cdot \boldsymbol{w}$ must be treated specifically. A lot of non-oscillatory schemes for conservation laws have been developed to solve this problem [11, 14, 19]. Such schemes consider a polynomial reconstruction of the sought function on cells and discretize the intermediate value of this function at the cell's boundaries. The involved derivatives of the transported quantity are computed with high orders accurate difference scheme. The value of these derivatives are attenuated through limiting function (so called slope limiters). This prevents from inappropriate numerical error amplifications. The ENO (Essentially non-oscillatory) or WENO (Weighted ENO) constitute the most used schemes of such family[16, 21].

To achieve an accurate and stable discretization of the advective term, one must use conservative numerical scheme. Such schemes exactly respect the conservation law within the cell by integrating the flux value at cell boundaries.

Total Variation Diminishing (TVD) scheme (which are monotonicity preserving flux) prevents from an increase of oscillations over time and enables to transport shocks. All these methods are well detailed in [21].

Reconstruction of the vorticity In our work, the reconstruction of the vorticity on the cell boundaries is realized through a second order accurate method [17] based on a *Min-Mod limiter* on the regular spatial grid $(i\Delta_x, j\Delta_y)$:

$$\xi^+_{i+\frac{1}{2},j} = \xi_{i+1,j} - \frac{\Delta_x}{2}(\xi_x)_{i+1,j} \qquad \text{and} \qquad \xi^-_{i+\frac{1}{2},j} = \xi_{i,j} + \frac{\Delta_x}{2}(\xi_x)_{i,j},$$

$$\text{with } (\xi_x)_{i,j} = Minmod\left(2\frac{(\xi_{i,j}-\xi_{i-1,j})}{\Delta_x}, \frac{\xi_{i+1,j}-\xi_{i-1,j}}{2\Delta_x}, 2\frac{(\xi_{i+1,j}-\xi_{i,j})}{\Delta_x}\right),$$

$$\text{and } Minmod(x_1,\cdots,x_n) = \begin{cases} \inf_i(x_i) \text{ if } x_i \geq 0 \ \ \forall i \\ \sup_i(x_i) \text{ if } x_i \leq 0 \ \ \forall i \\ 0 \qquad \text{otherwise.} \end{cases}$$

The intermediate values $\xi^+_{i,j+\frac{1}{2}}$ and $\xi^-_{i,j+\frac{1}{2}}$ are computed in the same way. As the Mid-Mod limiter provides the smallest slope, the reconstructed values of the vorticity on the cell boundaries attenuate amplification effect due to spatial discontinuities.

Vorticity-velocity scheme To deal with the advective term, we use the following semidiscrete central scheme [13, 14]:

$$\partial_t \xi_{i,j} = -\frac{H^x_{i+\frac{1}{2},j}(t) - H^x_{i-\frac{1}{2},j}(t)}{\Delta_x} - \frac{H^y_{i,j+\frac{1}{2}}(t) - H^y_{i,j-\frac{1}{2}}(t)}{\Delta_y} + \nu_\xi D_{i,j}, \tag{21}$$

with a numerical convection flux derived from the monotone Lax-Friedricks flux:

$$\begin{aligned} H^x_{i+\frac{1}{2},j}(t) &= \frac{u_{i+\frac{1}{2},j}(t)}{2}\left[\xi^+_{i+\frac{1}{2},j} + \xi^-_{i+\frac{1}{2},j}\right] - \frac{|u_{i+\frac{1}{2},j}(t)|}{2}\left[\xi^+_{i+\frac{1}{2},j} - \xi^-_{i+\frac{1}{2},j}\right] \\ H^y_{i,j+\frac{1}{2}}(t) &= \frac{v_{i,j+\frac{1}{2}}(t)}{2}\left[\xi^+_{i,j+\frac{1}{2}} + \xi^-_{i,j+\frac{1}{2}}\right] - \frac{|v_{i,j+\frac{1}{2}}(t)|}{2}\left[\xi^+_{i,j+\frac{1}{2}} - \xi^-_{i,j+\frac{1}{2}}\right]. \end{aligned} \tag{22}$$

This resulting second order, semidiscrete central scheme is TVD [13, 17] and not very dissipative. The intermediate values of the velocities are computed with a fourth-order averaging:

$$\begin{aligned} u_{i+\frac{1}{2},j}(t) &= \frac{-u_{i+2,j}(t) + 9u_{i+1,j}(t) + 9u_{i,j}(t) - u_{i-1,j}(t)}{16} \\ v_{i,j+\frac{1}{2}}(t) &= \frac{-v_{i,j+2}(t) + 9v_{i,j+1}(t) + 9v_{i,j}(t) - v_{i,j-1}(t)}{16}. \end{aligned} \tag{23}$$

The linear viscosity $\Delta\xi$ is approximated by the fourth-order central differencing:

$$\begin{aligned} D_{i,j}(t) = &\frac{-\xi_{i+2,j}(t) + 16\xi_{i+1,j}(t) - 30\xi_{i,j}(t) + 16\xi_{i-1,j}(t) - \xi_{i-2,j}(t)}{12\Delta_x^2} \\ &+ \frac{-\xi_{i,j+2}(t) + 16\xi_{i,j+1}(t) - 30\xi_{i,j}(t) + 16\xi_{i,j-1}(t) - \xi_{i,j-2}(t)}{12\Delta_y^2}. \end{aligned} \tag{24}$$

The time integration is realized with a third-order Runge Kutta scheme, which also respect the TVD property [21]. The divergence is integrated with a stable implicit discretization. The motion field is updated at each time step in the Fourier domain with equation (17). With this whole non-oscillatory scheme, the vorticity-velocity and divergence equations can be integrated in the image area.

Adjoint discretization Variational data assimilation assumes that the adjoint operator is the exact numerical adjoint of the direct operator [22]. Thus, the adjoint computation must be done according to the previously described vorticity simulation method. For large scale applications involving several coupled state variables of huge dimension and where for each of them a specific dynamical model is discretized accordingly, automatic differentiation programs [9] are used to compute the adjoint model. In our case, as only two variables are involved, it is possible to derive an explicit version of the discretized adjoint operator and a backward Runge-Kutta integration can be realized [10].

5 Results

In order to assess the benefits of our technique for the tracking of fluid motion, we first applied it on a synthetic sequence of particles images of a 2D divergence free turbulence obtained through a direct numerical simulation of the Navier-Stokes equation [2]. In this sequence composed of 52 images, we compare in figure 1 the vorticity map of the actual, the observed and the assimilated motion fields. It

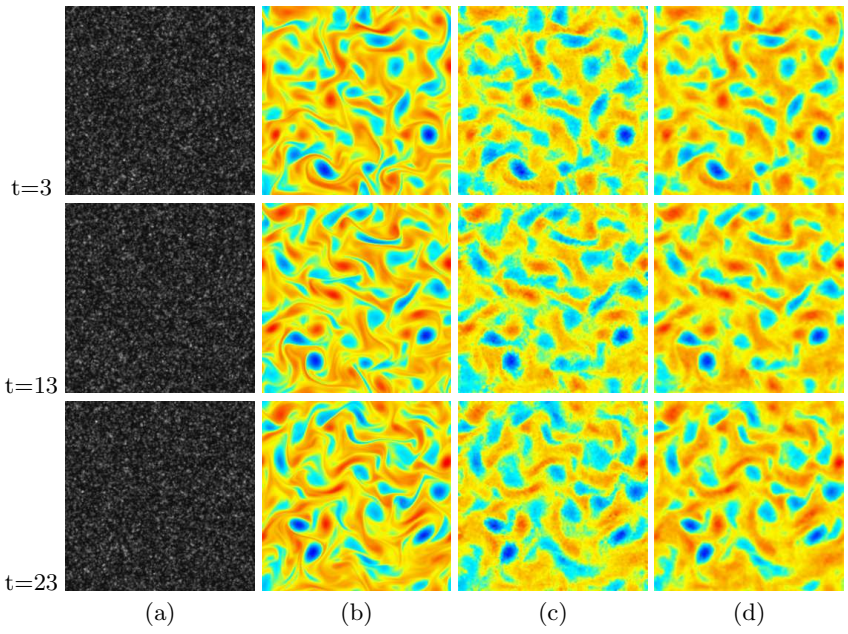

Fig. 1. 2D Direct Numerical Simulation. *a)* Particle images sequence. *b)* True vorticity. *c)* Vorticity observed by optic flow estimator. *d)* Recovered vorticity.

can be observed that the proposed technique not only denoises the observations, but also enables to recover small scales structures that were smoothed out in the original velocity fields. These observations were obtained from a dedicated optic flow estimator [3]. To give some quantitative evaluation results, we present the comparative errors in figure 2. As can be seen, we have been able to significantly improve the quality of the recovered motion field (about 30%). A spectral analysis of the energy of the row average vorticity is also realized in order to show that our assimilation process recovers the high frequencies of the flow, which correspond to the small scales spatial structures.

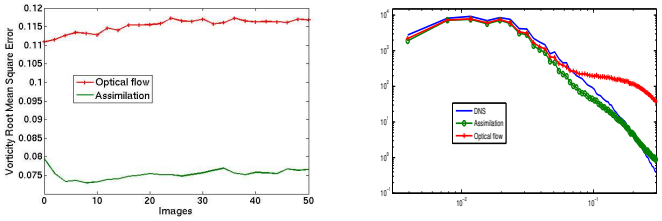

Root Mean Square Error Spectral analysis

Fig. 2. Comparison of errors. On the left figure, the red curve outlines the mean square error of the vorticity computed by the optic flow technique on the 25 images of the particle sequence. The green curve exhibits the error obtained at the end of the assimilation process. The assimilated vorticity is then closer to the reality than the observed one. The actual mean absolute value of the vorticity is about 0.43. On the right, a spectral analysis of the energy of the row average vorticity is represented in the log-log scale. Contrarily to the observed vorticity, the assimilated vorticity recovers high frequencies.

Finally, we applied our technique on a Infra-red meteorological sequence showing Vince cyclone over north atlantic. The sequence is composed by 20 satellite images acquired the 9 october 2005 from 00:00 up to 5:00 am[2]. Complete results in term of curves and vorticity maps are presented on figure 3. Line (b) exhibits the different vorticity maps of the initial motion fields used as noisy measurements. These motion observations present temporal inconsistencies and discontinuities, whereas the recovered vorticity maps shown on line (c) are more compliant with the vorticity conservation law.

6 Conclusion

In this work a variational framework for the tracking of fluid flows has been introduced. This approach relies on variational data assimilation principles. The proposed method allows to recover the state of an unknown function on the basis of an imperfect dynamical models and noisy measurement of this function. This technique has been applied to the tracking of fluid motion from image sequences.

[2] We thank the Laboratoire de Météorologie Dynamique for providing us this sequence.

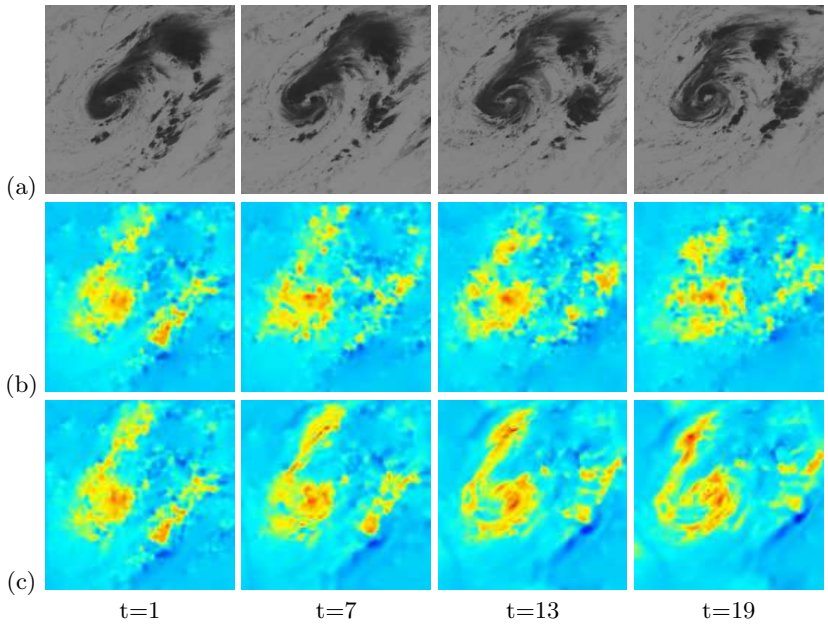

Fig. 3. Cyclone sequence. *(a)* Cyclone sequence. *(b)* Sample of observed vorticity maps. *(c)* Vorticity maps corresponding to the recovered motion fields.

Acknowledgments. This work was supported by the European Community through the IST FET Open FLUID project (`http://fluid.irisa.fr`).

References

1. A.F. Bennet. *Inverse Methods in Physical Oceanography.* Cambridge University Press, 1992.
2. J. Carlier and B. Wieneke. Report on production and diffusion of fluid mechanics images and data. Technical report, Fluid Project deliverable 1.2, 2005.
3. T. Corpetti, E. Mémin, and P. Pérez. Dense estimation of fluid flows. *IEEE Trans. Pattern Anal. Machine Intell.*, 24(3):365–380, 2002.
4. T. Corpetti, E. Mémin, and P. Pérez. Extraction of singular points from dense motion fields: an analytic approach. *J. Math. Imaging and Vision*, 19(3):175–198, 2003.
5. A. Cuzol and E. Mémin. A stochastic filter for fluid motion tracking. In *Int. Conf. on Computer Vision (ICCV'05)*, Beijing, China, October 2005.
6. F.-X. Le Dimet and O. Talagrand. Variational algorithms for analysis and assimilation of meteorological observations: theoretical aspects. *Tellus*, pages 97–110, 1986.
7. J.M. Fitzpatrick. A method for calculating velocity in time dependent images based on the continuity equation. In *Proc. Conf. Comp. Vision Pattern Rec.*, pages 78–81, San Francisco, USA, 1985.
8. R.M. Ford, R. Strickland, and B. Thomas. Image models for 2-d flow visualization and compression. *Graph. Mod. Image Proc.*, 56(1):75–93, 1994.

9. R. Giering and T. Kaminski. Recipes for adjoint code construction. *ACM Trans. Math. Softw.*, 24(4):437–474, 1998.
10. M. Giles. On the use of runge-kutta time-marching and multigrid for the solution of steady adjoint equations. Technical Report 00/10, Oxford University Computing Laboratory, 2000.
11. A. Harten, B. Engquist, S. Osher, and S. R. Chakravarthy. Uniformly high order accurate essentially non-oscillatory schemes, 111. *J. of Comput. Phys.*, 71(2):231–303, 1987.
12. T. Kohlberger, E. Mémin, and C. Schnörr. Variational dense motion estimation using the helmholtz decomposition. In *Int. conf on Scale-Space theories in Computer Vision (Scale-Space'03)*, volume 2695, pages 432–448, Isle of Skye, UK, june 2003.
13. A. Kurganov and D. Levy. A third-order semidiscrete central scheme for conservation laws and convection-diffusion equations. *SIAM J. Sci. Comput.*, 22(4):1461–1488, 2000.
14. A. Kurganov and E. Tadmor. New high-resolution central schemes for nonlinear conservation laws and convetion-diffusion equations. *J. Comput. Phys.*, 160(1):241–282, 2000.
15. R. Larsen, K. Conradsen, and B.K. Ersboll. Estimation of dense image flow fields in fluids. *IEEE trans. on Geosc. and Remote sensing*, 36(1):256–264, Jan. 1998.
16. D. Levy, G. Puppo, and G. Russo. A third order central weno scheme for 2d conservation laws. *Appl. Num. Math.: Trans. of IMACS*, 33(1–4):415–421, 2000.
17. D. Levy and E. Tadmor. Non-oscillatory central schemes for the incompressible 2-d euler equations. *Math. Res. Let*, 4:321–340, 1997.
18. E. Mémin and P. Pérez. Fluid motion recovery by coupling dense and parametric motion fields. In *Int. Conf. on Computer, ICCV'99*, pages 620–625, 1999.
19. H. Nessyahu and E. Tadmor. Non-oscillatory central differencing for hyperbolic conservation laws. *J. of Comput. Phys.*, 87(2):408–463, 1990.
20. B. Oksendal. *Stochastic differential equations*. Spinger-Verlag, 1998.
21. C.-W. Shu. Essentially non-oscillatory and weighted essentially non-oscillatory schemes for hyperbolic conservation laws. *Advanced Numerical Approximation of Nonlinear Hyperbolic Equations, Lecture Notes in Mathematics*, 1697:325–432, 1998.
22. O. Talagrand. *Variational assimilation. Adjoint equations*. Kluwer Academic Publishers, 2002.
23. O. Talagrand and P. Courtier. Variational assimilation of meteorological observations with the adjoint vorticity equation. I: Theory. *J. of Roy. Meteo. soc.*, 113:1311–1328, 1987.
24. J. Yuan, P. Ruhnau, E. Mémin, and C. Schnörr. Discrete orthogonal decomposition and variational fluid flow estimation. In *5th Int. Conf. on Scale-Space and PDE methods in Computer Vision (Scale-Space'05), Hofgeismar, Germany*, April 2005.
25. J. Yuan, C. Schnörr, and E. Mémin. Discrete orthogonal decomposition and variational fluid flow estimation. *Accepted for publication in J. of Math. Imaging and Vision*, 2006.
26. L. Zhou, C. Kambhamettu, and D. Goldgof. Fluid structure and motion analysis from multi-spectrum 2D cloud images sequences. In *Proc. Conf. Comp. Vision Pattern Rec.*, volume 2, pages 744–751, Hilton Head Island, USA, 2000.